THE JOURNAL OF BIOLOGICAL CHEMISTRY VOL. 281, NO. 15, pp. 10555–10560, April 14, 2006
Printed in the U.S.A.

The Mammalian Longevity-associated Gene Product p66^{shc} Regulates Mitochondrial Metabolism*[S]

Received for publication, October 26, 2005, and in revised form, February 7, 2006 Published, JBC Papers in Press, February 14, 2006, DOI 10.1074/jbc.M511626200

Shino Nemoto[‡], Christian A. Combs[§], Stephanie French[¶], Bong-Hyun Ahn[‡], Maria M. Fergusson[‡], Robert S. Balaban[¶], and Toren Finkel[‡1]

From the [‡]Cardiology Branch, NHLBI, National Institutes of Health, Bethesda, Maryland 20892-1622, [§]NHLBI, National Institutes of Health, Light Microscopy Facility, Bethesda, Maryland 20892, and the [¶]Laboratory of Cardiac Energetics, NHLBI, National Institutes of Health, Bethesda, Maryland 20892

Previous studies have determined that mice with a homozygous deletion in the adapter protein p66^{shc} have an extended life span and that cells derived from these mice exhibit lower levels of reactive oxygen species. Here we demonstrate that a fraction of p66^{shc} localizes to the mitochondria and that p66$^{shc-/-}$ fibroblasts have altered mitochondrial energetics. In particular, despite similar cytochrome content, under basal conditions, the oxygen consumption of spontaneously immortalized p66$^{shc-/-}$ mouse embryonic fibroblasts were lower than similarly maintained wild type cells. Differences in oxygen consumption were particularly evident under chemically uncoupled conditions, demonstrating that p66$^{shc-/-}$ cells have a reduction in both their resting and maximal oxidative capacity. We further demonstrate that reconstitution of p66^{shc} expression in p66$^{shc-/-}$ cells increases oxygen consumption. The observed defect in oxidative capacity seen in p66$^{shc-/-}$ cells is partially offset by augmented levels of aerobic glycolysis. This metabolic switch is manifested by p66$^{shc-/-}$ cells exhibiting an increase in lactate production and a stricter requirement for extracellular glucose in order to maintain intracellular ATP levels. In addition, using an *in vivo* NADH photobleaching technique, we demonstrate that mitochondrial NADH metabolism is reduced in p66$^{shc-/-}$ cells. These results demonstrate that p66^{shc} regulates mitochondrial oxidative capacity and suggest that p66^{shc} may extend life span by repartitioning metabolic energy conversion away from oxidative and toward glycolytic pathways.

Generation of ATP in the mitochondria represents the most efficient pathway to meet the energetic needs of a cell. This process, however, requires the consumption of molecular oxygen with a corresponding production of reactive oxygen species (ROS).[2] Generation of ROS appears to be one of the central mechanisms that contribute to aging in a wide range of organisms (1–3). In contrast, under aerobic conditions, energy generation can also be achieved through glycolytic pathways present in the cytosol. These cytosolic pathways are inherently less efficient but do not produce ROS. Each cell employs a different relative balance between these two major energetic pathways, although relatively little is known about how this partition is established or maintained.

In lower organisms, such as *Caenorhabditis elegans* and *Drosophila*, a number of longevity-associated genes have been isolated. One prominent and well characterized aging pathway regulates the activity of the transcription factor DAF-16, a member of the Forkhead family of transcriptional regulators. Evidence suggests that DAF-16 is involved in responding to numerous environmental stresses (4). A rise in intracellular ROS is one particular stress that may be relevant to life span determination, and in this regard, it is of interest that both DAF-16 and its closest mammalian ortholog Foxo3a appear to regulate a number of cellular antioxidant proteins (5–9).

In addition to the DAF-16 pathway, RNAi screens performed in *C. elegans* has identified a number of other putative longevity genes (10, 11). Interestingly, functional characterization of these longevity-associated genes have determined that a number of them appear to be important for mitochondrial function. Similarly, direct knockdown of components of the electron transport chain has also been shown to extend the life span of the worm (12). Analysis of these long lived mitochondrial mutants, as well as in depth energetic analysis of the previously characterized DAF-16-related mutants, has led to the proposal that many life span-extending mutants in *C. elegans* slow aging by decreasing mitochondrial metabolism (13). This hypothesis suggests that a shift away from trichloroacetic acid-based mitochondrial metabolism might extend life by a reduction in oxidative stress. Nonetheless, it should be mentioned that the relationship between metabolic rate and ROS production is not straightforward (3).

In contrast to the wealth of information regarding aging in lower organisms, there is relatively little known regarding the genetic control of mammalian life span. Only a handful of genes have to date been documented to be capable of extending either the mean or maximum age of mammalian organisms (14). One previously described knock-out mouse that appears to produce a long-lived but phenotypically normal animal was obtained after deletion of p66^{shc} (15). Shc proteins are alternatively spliced 46-, 52-, and 66-kDa isoforms that were initially viewed as simple adapter molecules linking receptors with downstream effector molecules such as Ras proteins (16). The larger p66^{shc} isoform differs structurally from its two other isoforms by the presence of a 14-kDa N-terminal CH2 domain. Previous studies have demonstrated that animals deficient in p66^{shc} have an approximate 30% extension in life span (15). These animals are resistant to exogenous oxidative stress and also exhibit lower levels of spontaneous oxidative burden (15, 17, 18). Consistent with these *in vivo* observations, p66$^{shc-/-}$ cells have lower levels of ROS (8, 19). One potential explanation for this effect may come from a modest increase in scavenging capacity in these cells (8); however, this is unlikely to explain the much more significant decrease in basal and stress-induced ROS levels.

* This work was supported by intramural funds from the National Institutes of Health. The costs of publication of this article were defrayed in part by the payment of page charges. This article must therefore be hereby marked "*advertisement*" in accordance with 18 U.S.C. Section 1734 solely to indicate this fact.

[S] The on-line version of this article (available at http://www.jbc.org) contains supplemental Figs. S1–S3.

[1] To whom correspondence should be addressed: National Institutes of Health, Bldg. 10/6N-240, 10 Center Dr., Bethesda, MD 20892-1622. Tel.: 301-402-4081; E-mail: finkelt@nih.gov.

[2] The abbreviations used are: ROS, reactive oxygen species; MEF, mouse embroyo fibroblast; FCCP, carbonylcyanide 4-(trifluoromethoxy)phenylhydrazone; ED-FRAP, enzyme-dependent fluorescence recovery after photobleaching.

Given that the mitochondria represent the largest source of ROS generation within cells and that oxygen consumption and ROS generation represent an important determinant in aging in a number of species, we sought to explore whether p66^{shc} might directly regulate ROS production by regulating mitochondrial metabolism.

MATERIALS AND METHODS

Cell Lines and Subcellular Fractionation—Spontaneously immortalized MEFs (+/+) cells and p66$^{shc-/-}$ MEFs were a gift of Pier Pelicci and have been previously described (8). PC12 and HeLa cells were obtained from ATCC (Rockville, MD). Cells were maintained in Dulbecco's modified Eagle's medium supplemented with 10% fetal calf serum. To purify the cytosolic and mitochondrial fractions, we used the ApoAlert Cell Fraction kit (Clontech). To assess the distribution of p66^{shc}, 30 μg of mitochondrial or cytosolic fractions were separated by SDS-PAGE, and the purity of the fractions was assessed by probing for the cytosolic gene product tubulin (Santa Cruz Biotechnology, Inc., Santa Cruz, CA) and the mitochondrial gene product COX4 (Clontech). For some experiments, we also collected and analyzed the initial 700 × *g* pellet containing plasma membranes. For construction of the R177A mutant, substitution of alanine for arginine residue at amino acid position 177 was performed by standard methods, and both the mutant and wild type were subsequently confirmed by direct sequencing. Reconstitution of p66^{shc} into p66$^{shc-/-}$ cells was achieved by transfection of the hygromycin resistance plasmid pTK-Hygro only for control cell lines or this resistance plasmid along with an epitope-tagged p66$^{shc-/-}$ expression plasmid that has been previously described (8). In both cases, hygromycin-resistant colonies were obtained, and p66^{shc} expression was monitored by Western blot analysis employing the epitope tag. For knock-down expression of p66^{shc} in PC12 cells, we targeted a 20-nucleotide sequence in p66^{shc}: GTACAACCCACTTCGGAATG. This sequence was incorporated into the psiRNA vector (InvivoGen) to enable the continuous, endogenous expression of small interfering RNAs in stable clones. For oxygen consumption measurements, two random knockdown cell lines were compared with two random Zeocin-selected PC12 cell lines transfected with the psiRNA vector alone.

Mitochondrial NADH and NADH Oxidase Measurements—Cellular NADH fluorescence was measured at room temperature using an excitation wavelength of 351 nm with emission monitored using a 385–470-nm band pass filter. Optical slice thickness was set to 1.5 μm. NADH regeneration was assessed using NADH ED-FRAP as previously described (20–22). In brief, all ED-FRAP data analysis was performed using custom-written programs in the IDL programming language (RSI Inc., Boulder, CO). Initial rates of regeneration were determined using a linear regression of the first five points (2 s) after the photolysis pulse. Before fitting, all recovery points were filtered using a Lee filter algorithm to smooth out additive image noise. To determine NADH consumption in cytosolic or mitochondrial fractions, MEF lysate was fractionated as above, and 30 μg of either mitochondrial or cytosolic lysate protein was used. Mitochondrial protein was solubilized in lysis buffer (20 mM Tris, pH 7.5, 0.5% Nonidet P-40, 25 mM NaCl, 2.5 mM EDTA) and subsequently diluted 1:20 (v/v) in phosphate buffer (pH 7.5), and the disappearance of 100 μM NADH was monitored at 340 nm.

Metabolic Measurements—Oxygen consumption was measured using an oxygen electrode standardized to room air (0.2 mM O_2). The data were digitized and stored using an analog to digital conversion system (DASYLab32). All measurements of oxygen consumption were performed in intact cells. In general, one representative experiment performed in triplicate is shown. All oxygen consumption experiments were performed on at least three separate occasions. To maximize oxygen consumption, the chemical uncoupler carbonylcyanide 4-(trifluoromethoxy)phenylhydrazone (FCCP; 5.0 μM) was used. Lactate was measured using the lactate reagent kit (Sigma). Media from wild type MEFs or p66$^{shc-/-}$ cells (1×10^6) were conditioned for 24 h prior to lactate determination. For the simultaneous determination of oxygen utilization and lactate levels, we employed the methods previously described (23). The degree of proton leak was calculated by measuring oxygen consumption in permeabilized cells (digitonin, 250 μg/ml) in the presence of oligomycin (25 μg/ml). ATP was measured from 1×10^6 cells using the ATP determination kit (Molecular Probes, Inc., Eugene, OR) with cells either maintained in full media or in media lacking glucose. Six hours after glucose withdrawal, cells were lysed in buffer (20 mM Tris, pH 7.5, 0.5% Nonidet P-40, 25 mM NaCl, 2.5 mM EDTA) for ATP determination. Results of ATP and lactate levels are, except where indicated, the results of a single representative experiment performed in triplicate. All experiments were performed at least three separate times.

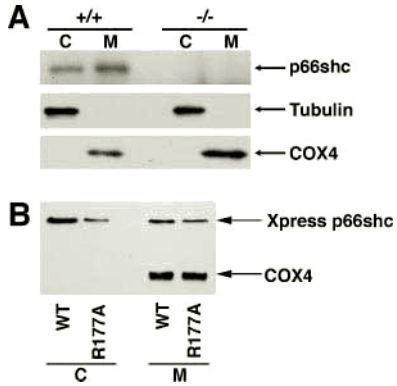

FIGURE 1. **A fraction of p66^{shc} is associated with the mitochondria.** *A*, subcellular fractionation of cytosolic (*C*) or mitochondrial (*M*) fractions were prepared from wild type (+/+) or p66$^{shc-/-}$ mouse embryonic fibroblasts. Each lane contained 30 μg of protein. The purity of the fractions was confirmed by assessing the distribution of the cytosolic protein tubulin and the mitochondrial protein cytochrome oxidase subunit 4 (*COX4*). *B*, subcellular distribution of wild type (*WT*) Xpress-tagged p66^{shc} or a site-directed position 177 mutant (R177A) following transient transfection of HeLa cells.

RESULTS

p66^{shc} Localizes to the Mitochondria and Regulates Oxygen Consumption and Oxidative Capacity—Since Shc proteins were viewed as adapter molecules for cell surface receptor complexes, the subcellular localization of p66^{shc} as well as its two other protein isoforms, p46^{shc} and p52^{shc}, were initially thought to be confined to the plasma membrane. Recent reports have challenged this assumption, and in particular evidence suggests that p46^{shc} localizes exclusively to the mitochondria and that a 32-amino acid motif is essential for this targeting (24). This 32-amino acid motif is not unique for p46^{shc} and is also contained within p66^{shc}. Consistent with these observations, recent evidence suggests that this larger Shc isoform might also be partially localized within the mitochondria (24, 25). As noted in Fig. 1, we also observed that a proportion of p66^{shc} was consistently found within the mitochondrial fraction. Based on calculation of the relative mass of the mitochondrial fraction, we estimate that ~10% of p66^{shc} is contained within the mitochondria of our wild type MEFs. This estimation is in good agreement with other recent observations (25) as well as indirect immunofluorescence data (supplemental Fig. S1).

As mentioned above, importation of p46^{shc} into the mitochondria requires a nonconventional N-terminal 32-amino acid targeting sequence and, in particular, an arginine residue at position 22 of the protein (24). This entire targeting sequence is also contained within the p66^{shc} isoform, but because of the N-terminal CH2 domain of p66^{shc}, the

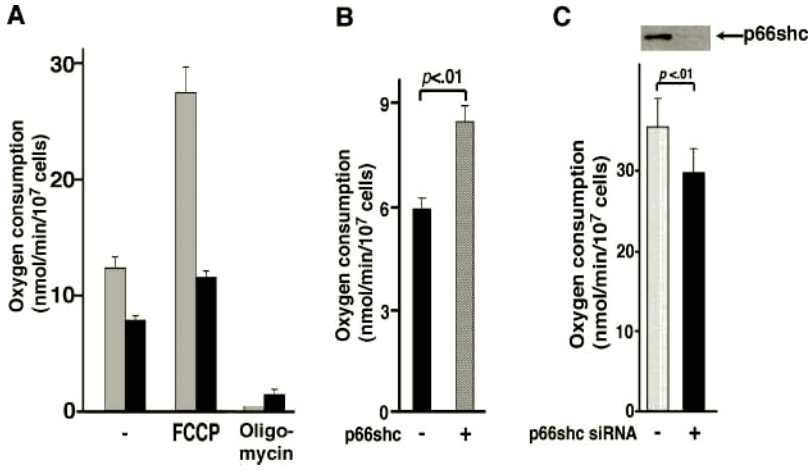

FIGURE 2. **The role of p66^{shc} in oxygen consumption.** *A*, levels of oxygen consumption in one of three similar experiments comparing wild type MEFs (*gray bars*) and p66$^{shc-/-}$ cells (*black bars*). Oxygen consumption was measured in triplicate under base line conditions (−) or following chemical uncoupling with FCCP (5 μM) or in the presence of the mitochondrial inhibitor oligomycin. *B*, levels of oxygen consumption in seven random p66$^{shc-/-}$ stable cell lines transfected with an empty vector expressing hygromycin resistance alone (−), or seven random cell lines with reconstituted wild type p66^{shc} (+). *C*, PC12 cells with and without stable expression of a short interfering RNA directed at p66^{shc}. Mean oxygen consumption of two control and two knock-down cell lines each measured in duplicate are shown. *Inset*, expression levels of p66^{shc} in one representative control and knockdown PC12 cell line.

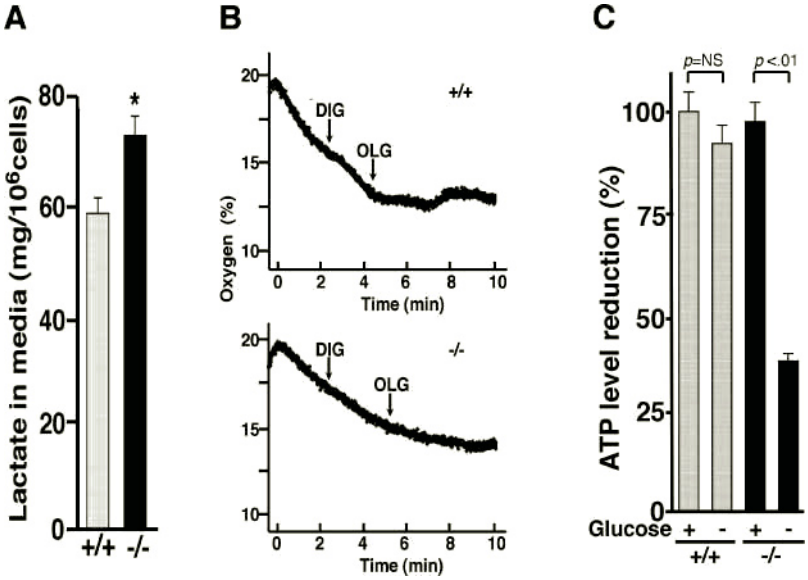

FIGURE 3. **p66$^{shc-/-}$ MEFs have altered levels of lactate production.** *A*, levels of lactate in media conditioned for 24 h by either wild type (+/+) or p66$^{shc-/-}$ cells. *, $p < 0.02$. *B*, levels of oligomycin-insensitive respiration in wild type and p66$^{shc-/-}$ cells. Real time oxygen consumption of intact wild type (+/+) and p66$^{shc-/-}$ cells. The addition of the permeabilizing agent digitonin (*DIG*) did not materially effect oxygen consumption, whereas the addition of oligomycin (25 μg/ml) dramatically reduced respiration in wild type and p66$^{shc-/-}$ cells. *C*, levels of ATP in wild type MEFs (+/+) or p66$^{shc-/-}$ cells at base line or 6 h after glucose withdrawal.

critical arginine reside occurs at position 177. Making the corresponding Arg^{177} substitution in p66^{shc} revealed that this amino acid change did not significantly alter the distribution of p66^{shc} (Figs. 1*B* and S1). Thus, importation of p66^{shc} into the mitochondria appears to occur via a mechanism that significantly diverges from the p46^{shc} isoform.

We next sought to understand whether the absence of p66^{shc} in cells alters mitochondrial function. Given the relationship between mitochondrial metabolism and aging, we first sought to characterize oxygen consumption in intact wild type and p66$^{shc-/-}$ cells. As noted in Fig. 2*A*, basal oxygen consumption was reduced by ~30–50% in p66$^{shc-/-}$ MEFs. This difference could not be explained by differences in mitochondrial number, since cytochrome *a* and a_3 content was similar in the two cell types (wild type MEFs, 40 ± 8 μmol/10^7 cell; p66$^{shc-/-}$ MEFs, 50 ± 5 μmol/10^7 cell, *p* not significant). In an effort to measure maximal oxygen consumption, we treated cells with the chemical uncoupling agent FCCP. Oxygen consumption of wild type and p66$^{shc-/-}$ MEFs treated with FCCP demonstrated a bell-shaped concentration effect with maximal uncoupling noted at 5 μM FCCP, a concentration that was subsequently employed in all experiments. As noted in Fig. 2*A*, under these maximally uncoupled conditions, wild type cells more than doubled their oxygen consumption, whereas p66$^{shc-/-}$ cells had a much more modest rise in oxygen consumption. In contrast, the addition of the mitochondrial inhibitor oligomycin resulted in a similar and nearly complete reduction in oxygen consumption in both wild type and p66$^{shc-/-}$ cells. Therefore, under resting conditions, oxygen consumption in both cell types appears to derive almost exclusively from mitochondrial cytochrome chain activity, and the degree of oligomycin-insensitive uncoupled respiration appears low.

To further confirm the role of p66^{shc} in regulating oxygen consumption, we generated stable cell lines with reconstituted p66^{shc} in an MEF knock-out cell background. Seven random control clones of p66$^{shc-/-}$ transfected with an empty vector had levels of oxygen consumption similar to what was previously observed in the p66$^{shc-/-}$ parental cell line (Fig. 2*B*). In contrast, seven random clones transfected with a p66^{shc} expression vector had increased levels of oxygen consumption ($p < 0.01$). This difference in respiration did not appear to reflect differences in uncoupling, since the level of oligomycin-insensitive respiration did not appreciably differ between the p66^{shc}-reconstituted and empty vector clones (supplemental Fig. S2). To potentially extend these observations to other cell types, we also created stable clones of PC12 cells constitutively expressing a short interfering RNA directed at p66^{shc}. Compared with two control PC12 lines, PC12 cells with knock-down p66^{shc} expression had reduced oxygen consumption (Fig. 2*C* and *inset*).

Absence of p66^{shc} Increases Aerobic Glycolysis—If p66$^{shc-/-}$ cells have less oxygen consumption and hence less mitochondria-dependent energy generation, then presumably energetic demands are met through an increase in alternative ATP-generating pathways. One major alternative pathway is aerobic glycolysis, with the ATP-generating step deriving from

TABLE 1

Sources of ATP generation in wild type (+/+) and p66$^{shc-/-}$ MEFs

Percentage of ATP derived from mitochondrial respiration is decreased in p66$^{shc-/-}$ cells. Calculations are based on the level of coupled respiration and aerobic glycolysis in both cell types according to previous methods (23).

	O_2 consumption	Lactic acid	Total ATP	Percentage of ATP production from	
				Respiration	Glycolysis
	nmol/min/mg protein			%	%
+/+	2.3 ± 0.3	10 ± 0.9	24 ± 1.5	54.1	45.9
−/−	1.4 ± 0.1	14 ± 1.4	22 ± 1.6	35.0	65.0

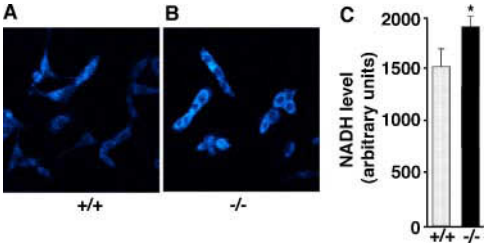

FIGURE 4. **p66^{shc} alters NADH levels.** Shown is endogenous NADH fluorescent intensity in wild type cells (*A*) or in p66$^{shc-/-}$ cells (*B*). *C*, quantification in arbitrary units of NADH fluorescent intensity. Data represent the mean ± S.D. from 25 random wild type or p66$^{shc-/-}$ cells. *, $p < 0.05$.

the cytosolic conversion of pyruvate to lactate. Measurement of 24-h lactate production revealed that p66$^{shc-/-}$ cells did indeed have evidence for increased lactate production (Fig. 3*A*). To understand the relative balance between aerobic respiration occurring in the mitochondria and glycolysis taking place within the cytosol, we simultaneously measured oxygen consumption and lactate levels using a previously described method (23). As noted in Table 1, using these values, as well as the calculated level of proton leak derived from oligomycin-insensitive respiration (Fig. 3*B*), we determined that wild type MEFs had over half of their ATP production derived from aerobic respiration. In contrast, for p66$^{shc-/-}$ cells, aerobic respiration accounted for closer to one-third of ATP production.

The increased reliance on glycolysis for p66$^{shc-/-}$ cells was also demonstrated by the differences in energetic homeostasis in the setting of glucose withdrawal. Under these conditions, oxidative phosphorylation is supported by the remaining carbon substrates, most notably glutamate and fatty acids. As noted in Fig. 3*C*, 6 h after withdrawing glucose from the media, wild type cells had a modest, but not statistically significant, fall in intracellular ATP levels. In contrast, the same glucose withdrawal resulted in a pronounced reduction in intracellular ATP levels in p66$^{shc-/-}$ cells. These results are consistent with the classical Pasteur effect, whereby an inhibition of oxidative metabolism results in an increased reliance on less efficient, glycolytic pathways to meet cellular energetic demands.

Regulation of Mitochondrial NADH Metabolism by p66^{shc}—We next sought to further understand the basis for the difference in resting oxygen consumption between wild type and p66$^{shc-/-}$ MEF. As noted in Fig. 4, *A* and *B*, microfluorometric measurements of the distribution of NADH appeared similar in wild type and p66$^{shc-/-}$ cells. This technique predominantly measures protein-bound NAD(P)H and is therefore most reflective of mitochondrial rather then free cytosolic NAD(P)H levels. Quantification of the NADH fluorescent intensity revealed an approximate 20% increase in resting fluorescence in knock-out cells (Fig. 4*C*). Since the interpretation of resting NADH levels in quiescent cells is difficult, we next sought to assess whether differences existed in NADH turnover between these two cell types. Using a previously

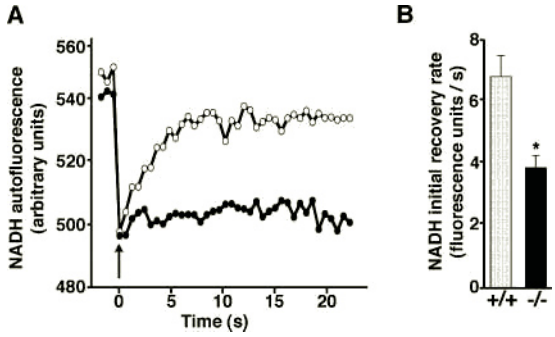

FIGURE 5. **p66^{shc} alters mitochondrial NADH flux.** *A*, representative NADH ED-FRAP time course from a single wild type (*open circles*) or p66$^{shc-/-}$ cell (*closed circles*). The *arrow* indicates the timing of the photolysis pulse. *B*, composite analysis of the level of initial NADH recovery (first 2 s) following NADH to NAD photolysis in individual wild type (*open bar*, $n = 11$) and p66$^{shc-/-}$ (*shaded bar*, $n = 10$) cells. *, $p < 0.03$.

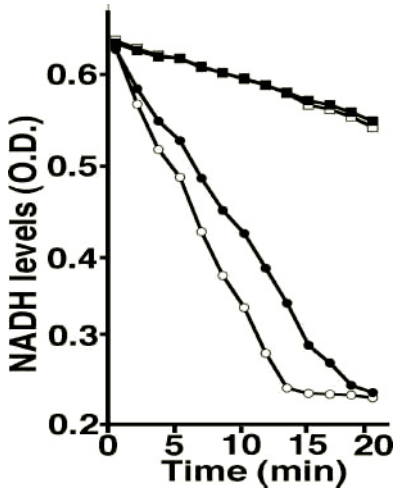

FIGURE 6. **Permeabilized p66^{shc} mitochondria have reduced NADH consumption.** Measurement of *in vitro* consumption of exogenous NADH using either cytosolic (*squares*) or permeabilized mitochondrial (*circles*) extracts from wild type MEFs (*open symbols*) or p66$^{shc-/-}$ cells (*closed symbols*). Whereas cytosolic consumption of NADH is indistinguishable, consumption of exogenous NADH is reduced for p66$^{shc-/-}$ mitochondria.

described NADH photolysis technique, NADH ED-FRAP (20–22), we noted that p66$^{shc-/-}$ cells exhibited an overall reduction in the degree of NADH regeneration following the laser-induced photolysis of NADH to NAD (Fig. 5*A*). Quantification of the initial recovery rate of NADH regeneration following photolysis demonstrated an approximate 40% reduction in p66$^{shc-/-}$ cells (Fig. 5*B*). These data are consistent with p66$^{shc-/-}$ cells having a blockage or slowing of NADH synthesis from NAD, a process that normally occurs either in the Krebs cycle or from reverse electron flow through Site I of oxidative phosphorylation (21).

Whereas the experiments employing ED-FRAP are most consistent with a defect in mitochondrial NADH metabolism, we could not exclude a contribution from less abundant cytosolic NADH-regenerating enzymes. Therefore, to further pursue the question of alterations in NADH metabolism, we prepared cytosolic and mitochondrial extracts from wild type and p66$^{shc-/-}$ cells. As noted in Fig. 6, cytosolic consumption of exogenous NADH was similar in the two cell lines. In contrast, compared with wild type cells, permeabilized mitochondria derived from p66$^{shc-/-}$ cells had a considerably slower rate of exogenous NADH consumption. As such, these biochemical measurements are consistent with the previously described noninvasive, NADH ED-FRAP measurements and suggest that the defect in NADH metabolism in p66^{shc} cells is confined predominantly to the mitochondria.

DISCUSSION

The identification of gene products that regulate life span has provided significant insight into the molecular mechanisms that underlie aging. In contrast to lower organisms, to date, only a handful of mammalian longevity genes have been identified, and it remains unclear as to how these gene products actually regulate life span (14). One dominant theory regarding aging involves the role of overall metabolism and, in particular, the contribution of reactive oxygen species generated by mitochondrial metabolism (1–3). Here we have demonstrated that the mammalian longevity gene product p66^{shc} functions as a regulator of mitochondrial metabolism.

The impetus for our investigation began with the initial observation that p66$^{shc-/-}$ mice exhibit increased resistance to oxidative stress such as was observed following paraquat exposure (15). There is also evidence that animals lacking p66^{shc} have a reduction in other markers of basal oxidative stress (17, 18). Consistent with these observations, cells derived from p66^{shc} animals have reduced resting and stress-induced levels of ROS (8, 19). In the process of performing these experiments, a very recent report suggested that p66^{shc} can generate hydrogen peroxide in conjunction with reduced cytochrome *c* (25). These authors have argued that this property is essential for the burst of mitochondrial ROS that occurs with the induction of apoptosis. Interestingly, this study identified a region of p66^{shc} required for the *in vitro* interaction with cytochrome *c* that is adjacent to but outside the unique CH2 domain of the protein. Since this identified region is also present in p52^{shc}, it is unclear whether this ROS-producing property is also shared by the other Shc isoforms that are not currently associated with longevity. It also remains unclear how this ability to generate hydrogen peroxide following apoptotic stress relates to the observation that levels of ROS are chronically reduced in p66$^{shc-/-}$ cells and animals, especially since under basal conditions, one would not expect a significant rate of apoptosis. One possibility is that nonapoptotic stresses could also activate p66^{shc} to produce hydrogen peroxide in a cytochrome *c*-dependent fashion. Although answers to these questions require further study, together they argue that p66^{shc} has properties beyond being a simple adapter molecule.

Whereas our data and previous studies suggest that a fraction of p66^{shc} localizes to the mitochondria, it is currently unclear how this importation occurs. In the related p46^{shc} molecule, an N-terminal stretch of 32 amino acids is responsible for directing this isoform exclusively to the mitochondria (24). This sequence is not recognized by current bioinformatic methods as a mitochondrial targeting sequence. Within this region, arginine 22 is essential for mitochondrial targeting (24). The corresponding 32-amino acid stretch is found in p66^{shc}, but as demonstrated here and previously, the majority of p66^{shc} is nonmitochondrial. Similarly, as we show here, in contrast to the p46^{shc} isoform, mutation of the corresponding arginine in p66^{shc} does not alter the subcellular distribution of the protein. It remains possible that our localization of p66^{shc} within the mitochondria is spurious and that the mitochondrial fractions used in our subcellular fractionation experiments were contaminated in some fashion, perhaps by the inadvertent inclusion of plasma membranes. Although this remains a possibility, several observations argue against this. First, previous experiments using perhaps the gold standard of subcellular localization, immunogold electron microscopy, have consistently detected p66^{shc} within the mitochondria (25, 26). Similarly, p66^{shc} has been shown to form a molecular complex with the mitochondrial protein cytochrome *c* (25). Finally, analysis of our fractions suggests that, at least at the level of Western blot detection, the mitochondrial fractions are relatively free of contamination (supplemental Fig. 3). Nonetheless, until more information is known regarding the mechanisms underlying mitochondrial localization, we cannot conclusively state that the metabolic effects seen in our p66$^{shc-/-}$ cells are due to the absence of p66^{shc} in the mitochondria rather then the absence of this protein in another subcellular compartment.

The observations presented here suggest that p66^{shc} may regulate the partition of ATP generation in the cell and that in the absence of p66^{shc}, mitochondrial oxidative phosphorylation is reduced, whereas the reliance on glycolysis is increased. Given that mitochondrial electron flow is the major producer of cellular ROS, these results may provide an explanation for the previous observation that p66$^{shc-/-}$ cells and animals have lower levels of ROS (8, 15, 17–19). It should be noted that our results were predominantly obtained in spontaneously immortalized MEFs. A similar albeit smaller role for p66^{shc} in regulating oxygen consumption was also seen in PC12 cells (Fig. 2*C*). Our preliminary observations of oxygen consumption in primary MEFs derived from p66$^{shc-/-}$ animals suggest that the metabolic alterations are significantly less then what we observed in our immortalized MEFs (data not shown). Thus, the role of p66^{shc} in mitochondrial metabolism may vary considerably between different cell types and even between primary and immortalized MEFs. Although considerable drift can occur with cell culture, the observation that reconstitution of p66^{shc} in our spontaneously immortalized knock-out MEFs increases oxygen consumption (Fig. 2*B*) provides strong evidence for a continuous role of p66^{shc} in the observed metabolic phenotype.

Although to date, relatively few mammalian longevity genes have been determined, there is a much richer literature from other species such as nematodes. Although the requirement for oxygen and the ability to withstand prolonged hypoxia clearly differs between worms and higher mammals, it is interesting to note that a number of previously described *C. elegans* longevity mutants have altered mitochondrial metabolism (10, 11). Included among these is the *isp-1* mutant, which has a defect in Complex III leading to decreased oxygen consumption and extended life (27). Similarly, RNAi methods have determined that inhibition of mitochondrial electron transport or other essential mitochondrial proteins can often result in worms that have reduced oxygen consumption, lower ATP levels, and a corresponding increase in life span (12). Thus, as recently hypothesized, reducing the level of mitochondrial metabolism may be an important way of extending the life span of lower organisms (13). The results presented here, along with previous studies demonstrating an extended life span of p66$^{shc-/-}$ mice (15), suggest that this paradigm may also be applicable to mammalian species.

Acknowledgment—We are grateful to P Pelicci for the gift of p66$^{shc-/-}$ MEFs.

REFERENCES

1. Finkel, T., and Holbrook, N. J. (2000) *Nature* **408,** 239–247
2. Wallace, D. C. (2005) *Annu. Rev. Genet.* **39,** 359–407
3. Balaban, R. S., Nemoto, S., and Finkel, T. (2005) *Cell* **120,** 483–495
4. Johnson, T. E., de Castro, E., Hegi de Castro, S., Cypser, J., Henderson, S., and Tedesco, P. (2001) *Exp. Gerontol.* **36,** 1609–1617
5. Murphy, C. T., McCarroll, S. A., Bargmann, C. I., Fraser, A., Kamath, R. S., Ahringer, J., Li, H., and Kenyon, C. (2003) *Nature* **424,** 277–283
6. Lee, S. S., Kennedy, S., Tolonen, A. C., and Ruvkun, G. (2003) *Science* **300,** 644–647
7. McElwee, J., Bubb, K., and Thomas, J. H. (2003) *Aging Cell* **2,** 111–121
8. Nemoto, S., and Finkel, T. (2002) *Science* **295,** 2450–2452
9. Kops, G. J., Dansen, T. B., Polderman, P. E., Saarloos, I., Wirtz, K. W., Coffer, P. J., Huang, T. T., Bos, J. L., Medema, R. H., and Burgering, B. M. (2002) *Nature* **419,** 316–321
10. Lee, S. S., Lee, R. Y., Fraser, A. G., Kamath, R. S., Ahringer, J., and Ruvkun, G. (2003) *Nat. Genet.* **33,** 40–48
11. Hamilton, B., Dong, Y., Shindo, M., Liu, W., Odell, I., Ruvkun, G., and Lee, S. S. (2005)

Genes Dev. **19,** 1544–1555
12. Dillin, A., Hsu, A. L., Arantes-Oliveira, N., Lehrer-Graiwer, J., Hsin, H., Fraser, A. G., Kamath, R. S., Ahringer, J., and Kenyon, C. (2002) *Science* **298,** 2398–2401
13. Rea, S., and Johnson, T. E. (2003) *Dev. Cell* **5,** 197–203
14. Kenyon, C. (2005) *Cell* **120,** 449–460
15. Migliaccio, E., Giorgio, M., Mele, S., Pelicci, G., Reboldi, P., Pandolfi, P. P., Lanfrancone, L., and Pelicci, P. G. (1999) *Nature* **402,** 309–313
16. Pelicci, G., Lanfrancone, L., Grignani, F., McGlade, J., Cavallo, F., Forni, G., Nicoletti, I., Pawson, T., and Pelicci, P. G. (1992) *Cell* **70,** 93–104
17. Napoli, C., Martin-Padura, I., de Nigris, F., Giorgio, M., Mansueto, G., Somma, P., Condorelli, M., Sica, G., De Rosa, G., and Pelicci, P. (2003) *Proc. Natl. Acad. Sci. U. S. A.* **100,** 2112–2116
18. Francia, P., delli Gatti, C., Bachschmid, M., Martin-Padura, I., Savoia, C., Migliaccio, E., Pelicci, P. G., Schiavoni, M., Luscher, T. F., Volpe, M., and Cosentino, F. (2004) *Circulation* **110,** 2889–2895
19. Trinei, M., Giorgio, M., Cicalese, A., Barozzi, S., Ventura, A., Migliaccio, E., Milia, E., Padura, I. M., Raker, V. A., Maccarana, M., Petronilli, V., Minucci, S., Bernardi, P., Lanfrancone, L., and Pelicci, P. G. (2002) *Oncogene* **21,** 3872–3878
20. Combs, C. A., and Balaban, R. S. (2001) *Biophys. J.* **80,** 2018–2028
21. Joubert, F., Fales, H. M., Wen, H., Combs, C. A., and Balaban, R. S. (2004) *Biophys. J.* **86,** 629–645
22. Combs, C. A., and Balaban, R. S. (2004) *Methods Enzymol.* **385,** 257–286
23. Sariban-Sohraby, S., Magrath, I. T., and Balaban, R. S. (1983) *Cancer Res.* **43,** 4662–4664
24. Ventura, A., Maccarana, M., Raker, V. A., and Pelicci, P. G. (2004) *J. Biol. Chem.* **279,** 2299–2306
25. Giorgio, M., Migliaccio, E., Orsini, F., Paolucci, D., Moroni, M., Contursi, C., Pelliccia, G., Luzi, L., Minucci, S., Marcaccio, M., Pinton, P., Rizzuto, R., Bernardi, P., Paolucci, F., and Pelicci, P. G. (2005) *Cell* **122,** 221–233
26. Orsini, F., Migliaccio, E., Moroni, M., Contursi, C., Raker, V. A., Piccini, D., Martin-Padura, I., Pelliccia, G., Trinei, M., Bono, M., Puri, C., Tacchetti, C., Ferrini, M., Mannucci, R., Nicoletti, I., Lanfrancone, L., Giorgio, M., and Pelicci, P. G. (2004) *J. Biol. Chem.* **279,** 25689–25695
27. Feng, J., Bussiere, F., and Hekimi, S. (2001) *Dev. Cell* **1,** 633–644